Cholinergic white matter pathways along the Alzheimer's disease continuum

Cholinergic white matter pathways along the Alzheimer's disease continuum

Milan Nemy,[1,2,3] Martin Dyrba,[4] Frederic Brosseron,[5] Katharina Buerger,[6,7] Peter Dechent,[8] Laura Dobisch,[9] Michael Ewers,[6,7] Klaus Fliessbach,[5,10] Wenzel Glanz,[9] Doreen Goerss,[4,11] Michael T. Heneka,[5,10] Stefan Hetzer,[12] Enise I. Incesoy,[9,13] Daniel Janowitz,[7] Ingo Kilimann,[4,11] Christoph Laske,[14,15] Franziska Maier,[16] Matthias H. Munk,[14,15] Robert Perneczky,[6,17,18,19,20] Oliver Peters,[21,22] Lukas Preis,[22] Josef Priller,[21,23,24,25] Boris-Stephan Rauchmann,[17] Sandra Röske,[5] Nina Roy,[5] Klaus Scheffler,[26] Anja Schneider,[5,10] Björn H. Schott,[27,28,29] Annika Spottke,[5,30] Eike J. Spruth,[21,23] Michael Wagner,[5,10] Jens Wiltfang,[27,28,31] Renat Yakupov,[9] Maria Eriksdotter,[3,32] Erik Westman,[3,33] Olga Stepankova,[2] Lenka Vyslouzilova,[2] Emrah Düzel,[9,13] Frank Jessen,[5,16,34] Stefan J. Teipel[4,11,†] and Daniel Ferreira[3,†]

[†]**These authors contributed equally to this work.**

Abstract

Previous studies have shown that the cholinergic nucleus basalis of Meynert and its white matter projections are affected in Alzheimer's disease (AD) dementia and mild cognitive impairment (MCI). However, it is still unknown if these alterations can be found in individuals with subjective cognitive decline (SCD), and whether they are more pronounced than changes found in conventional brain volumetric measurements. To address these questions, we investigated microstructural alterations of two major cholinergic pathways in individuals along the AD continuum using an *in vivo* model of the human cholinergic system based on neuroimaging.

We included 405 participants (53 AD, 66 MCI, 174 SCD, and 112 healthy controls) from the Deutsches Zentrum für Neurodegenerative Erkrankungen (DZNE) Longitudinal Cognitive Impairment and Dementia Study (DELCODE). We modelled the cholinergic white matter pathways with an enhanced diffusion neuroimaging pipeline that included probabilistic fiber-tracking methods and prior anatomical knowledge. The integrity of the cholinergic white matter pathways was compared between stages of the AD continuum, in the whole cohort and in a CSF amyloid-beta stratified subsample. The discriminative power of the integrity of the pathways was compared to the conventional volumetric measures of hippocampus and nucleus basalis of Meynert, using a receiver operating characteristics analysis. A multivariate model was employed to investigate the role of these pathways in relation to cognitive performance.

We found that the integrity of the cholinergic white matter pathways was significantly reduced in all stages of the AD continuum, including individuals with SCD. The differences involved posterior cholinergic white matter in the SCD stage and extended to anterior frontal white matter in MCI and AD dementia stages. Both cholinergic pathways and conventional volumetric measures showed higher predictive power in the more advanced stages of the disease, i.e., MCI and AD dementia. In contrast, the integrity of cholinergic pathways was more informative in distinguishing SCD from healthy controls, as compared with the volumetric measures. The multivariate model revealed a moderate contribution of the cholinergic white matter pathways but not of volumetric measures towards memory tests in the SCD and MCI stages.

In conclusion, we demonstrated that cholinergic white matter pathways are altered already in SCD individuals, preceding the more widespread alterations found in MCI and AD. The integrity of the cholinergic pathways identified the early stages of AD better than conventional

volumetric measures such as hippocampal volume or volume of cholinergic nucleus basalis of Meynert.

Author affiliations:

1 Department of Cybernetics, Faculty of Electrical Engineering, Czech Technical University in Prague, Prague, Czech Republic

2 Department of Biomedical Engineering and Assistive Technology, Czech Institute of Informatics, Robotics and Cybernetics, Czech Technical University in Prague, Prague, Czech Republic

3 Division of Clinical Geriatrics, Center for Alzheimer Research, Department of Neurobiology, Care Sciences and Society, Karolinska Institute, Stockholm, Sweden

4 German Center for Neurodegenerative Diseases (DZNE), Rostock, Germany

5 German Center for Neurodegenerative Diseases (DZNE), Bonn, Germany

6 German Center for Neurodegenerative Diseases (DZNE) Munich, Munich, Germany

7 Institute for Stroke and Dementia Research (ISD), University Hospital, LMU Munich, Munich, Germany

8 MR-Research in Neurosciences, Department of Cognitive Neurology, Georg-August-University Goettingen, Goettingen, Germany

9 German Center for Neurodegenerative Diseases (DZNE), Magdeburg, Germany

10 Department for Neurodegenerative Diseases and Geriatric Psychiatry, University Hospital Bonn, Bonn, Germany

11 Department of Psychosomatic Medicine, Rostock University Medical Center, Rostock, Germany

12 Berlin Center for Advanced Neuroimaging, Charité – Universitätsmedizin Berlin, Berlin, Germany

13 Institute of Cognitive Neurology and Dementia Research, Otto-von-Guericke University, Magdeburg, Germany

14 German Center for Neurodegenerative Diseases (DZNE), Tübingen, Germany

15 Section for Dementia Research, Hertie Institute for Clinical Brain Research and Department of Psychiatry and Psychotherapy, University of Tübingen, Tübingen, Germany

16 Department of Psychiatry, University of Cologne, Medical Faculty, Cologne, Germany

17 Department of Psychiatry and Psychotherapy, University Hospital, LMU Munich, Munich, Germany

18 Munich Cluster for Systems Neurology (SyNergy) Munich, Munich, Germany

19 Ageing Epidemiology Research Unit (AGE), School of Public Health, Imperial College London, London, UK

20 Sheffield Institute for Translational Neurosciences (SITraN), University of Sheffield, Sheffield, UK

21 German Center for Neurodegenerative Diseases (DZNE), Berlin, Germany

22 Charité-Universitätsmedizin Berlin, Campus Benjamin Franklin, Department of Psychiatry, Berlin, Germany

23 Department of Psychiatry and Psychotherapy, Charité, Berlin, Germany

24 Department of Psychiatry and Psychotherapy, School of Medicine, Technical University of Munich, Munich, Germany

25 University of Edinburgh and UK DRI, Edinburgh, UK

26 Department for Biomedical Magnetic Resonance, University of Tübingen, Tübingen, Germany

27 German Center for Neurodegenerative Diseases (DZNE), Goettingen, Germany

28 Department of Psychiatry and Psychotherapy, University Medical Center Goettingen, University of Goettingen, Goettingen, Germany

29 Leibniz Institute for Neurobiology, Magdeburg, Germany

30 Department of Neurology, University of Bonn, Bonn, Germany

31 Neurosciences and Signaling Group, Institute of Biomedicine (iBiMED), Department of Medical Sciences, University of Aveiro, Aveiro, Portugal

32 Theme Inflammation and Aging, Karolinska University Hospital, Stockholm, Sweden

33 Department of Neuroimaging, Centre for Neuroimaging Science, Institute of Psychiatry, Psychology, and Neuroscience, King's College London, London, UK

34 Excellence Cluster on Cellular Stress Responses in Aging-Associated Diseases (CECAD), University of Cologne, Cologne, Germany

Correspondence to: Daniel Ferreira

Division of Clinical Geriatrics, Center for Alzheimer Research, Department of Neurobiology, Care Sciences and Society, NEO floor 7th, Karolinska Institutet, 141 57, Huddinge, Stockholm, Sweden

E-mail: daniel.ferreira.padilla@ki.se

Running title: Cholinergic pathways in AD continuum

Keywords: cholinergic system; nucleus basalis of Meynert; Alzheimer's disease; cerebrospinal fluid markers; magnetic resonance imaging

Abbreviations: AD = Alzheimer's disease; ADAS = Alzheimer's Disease Assessment Scale; ANTs = Advanced Normalisation Tools; AUC = area under the ROC curve; Aβ = amyloid-beta; BF = basal forebrain; CSF = cerebrospinal fluid; DELCODE = Longitudinal Cognitive Impairment and Dementia Study; DTI = diffusion tensor imaging; EPI = echo-planar imaging; FA = fractional diffusivity; FAST = FSL's Automated Segmentation Tool; FSL = FMRIB Software Library; GDS = Geriatric Depression Scale; GM = gray matter; HC = healthy controls; MCI = mild cognitive impairment; MD = mean diffusivity; MMSE = Mini Mental State Examination; MRI = magnetic resonance imaging; NBM = nucleus basalis of Meynert; NFT = neurofibrillary tangle; NIA-AA = National Institute on Aging-Alzheimer's Association; RF = random forest; ROC = receiver operating characteristic; ROI = region of interest; SCD = subjective cognitive decline; SVD = small vessel disease; TFCE = threshold-free cluster enhancement; TIV = total intracranial volume; WM = white matter

Introduction

Current research in the field of Alzheimer's disease (AD)[1–3] suggests that pathological changes in the human brain can be observed decades before the onset of clinically detectable dementia.[4] Therefore, a disease continuum has been described, ranging from subjective cognitive decline (SCD) or preclinical AD to mild cognitive impairment (MCI) and fully developed dementia.[5] In the later stages of the continuum, major pathological and clinical changes are present, e.g., extracellular amyloid-beta (Aβ) plaques and intracellular neurofibrillary tangle (NFT) pathology, memory loss, and other cognitive alterations.[6] However, the brain changes taking place in the very early stages are less known. Capturing the earliest neurodegenerative changes is challenging because conventional quantitative biomarkers might not be sensitive enough.

Neurons in the hippocampus, basal forebrain (BF) and its subregion including the nucleus basalis of Meynert (NBM), are selectively vulnerable to AD pathology.[7] Both hippocampus and NBM are among the first brain structures to show signs of deterioration. They can be assessed through in vivo volumetric measurements based on magnetic resonance imaging (MRI).[8] Recent studies have shown that NBM volume is an earlier biomarker of AD-like neurodegeneration, as compared with the more conventional hippocampal volumetric measures.[9] This finding suggests that the loss of NBM neurons might be one of the earliest events of neurodegeneration in AD. The NBM and its cholinergic circuitry are heavily involved in cognitive decline characteristic of aging and age-related disorders, including AD.[10] Furthermore, neurons with long axonal connections are particularly susceptible to AD-related pathology.[11] These vulnerable groups of neurons seem to follow a dying-back pattern of degeneration, in which defects in myelinisation and synaptic dysfunction forego somatic cell death.[11] There is also evidence that the early white matter (WM) changes can be observed in vivo using diffusion MRI.[12,13] A recent study

demonstrated alterations in mean diffusivity of NBM WM projections in patients with AD and patients with MCI, using diffusion MRI.[14] What remains unknown is how cholinergic projections change in the preclinical stage of AD and how these changes relate to other common biomarkers.

The overall goal of the current study was to investigate neurodegeneration of the human cholinergic system using diffusion-weighted MRI across the stages of the AD continuum. We hypothesised that microstructural biomarkers (diffusion-based imaging indices) would detect signs of neurodegeneration earlier in the AD continuum than conventional volumetric measures (hippocampal and NBM volumes). Our first aim was to investigate differences in cholinergic WM pathways between stages of the AD continuum and a control group (healthy controls, HC), and to compare their predictive power to the volumetric measures. The second aim was to demonstrate the association of WM pathways and NBM volumetric changes with cognitive performance across stages of the AD continuum. As cognitive measures, we focused on attention and memory as they are known to be mediated by the cholinergic circuitry.[15] Our diagnostic groups of SCD, MCI, and AD dementia are clinically in the AD continuum but since they rely on a clinical diagnosis, it is possible that some individuals do not have an Alzheimer's pathologic change as defined currently by a positive amyloid-beta biomarker.[6] For this reason, to confirm our results in a biomarker-supported AD continuum subsample, we repeated all our analyses in a subsample of amyloid-positive SCD, MCI, and AD dementia groups, as well as amyloid-negative HC.

Materials and methods

Participants

We used data from the interim baseline data set of the multicenter DZNE-longitudinal Cognitive Impairment and Dementia Study (DELCODE), conducted by the German Center for Neurodegenerative Diseases (DZNE).[16] After excluding all cases with insufficient image quality, diffusion MRI data from 402 participants from ten centers were included (52 AD, 66 MCI, 172 SCD, and 112 HC). The participants underwent a clinical assessment of their cognitive status, including the Mini Mental State Examination (MMSE)[17] and an extensive neuropsychological testing battery as described previously.[16] Depressive symptoms were assessed with the Geriatric Depression Scale (GDS).[18] The DELCODE exclusion criteria are current major depressive episode, past or present major psychiatric disorders, neurological diseases other than AD or MCI, or unstable medical conditions.[16]

SCD was defined as a persistent self-perceived cognitive impairment in the absence of objective cognitive impairment, lasting at least for six months and being unrelated to an acute event.[19] The MCI patients met the core clinical criteria for MCI according to National Institute on Aging-Alzheimer's Association (NIA-AA) workgroup guidelines.[20] The AD patients had a clinical diagnosis of probable AD dementia according to the NIA-AA workgroup guidelines.[21] Additionally, for a subsample, we requested amyloid positivity for the SCD, MCI, and AD dementia groups.

The HC participants had no objective cognitive impairment in cognitive tests, no history of neurological or psychiatric disease, and did not report a self-perceived cognitive decline. For a subsample, we requested amyloid negativity for the HC group.

All participants or their legal representatives provided written informed consent. The study protocol was approved by the local institutional review boards and ethics committees of the participating centers. DELCODE was conducted in accord with the Helsinki Declaration of 1975.

Cognitive Assessment

DELCODE employs an extensive neuropsychological test battery covering specific domains of memory, executive functions, language, visuospatial abilities, as well as attention and working memory.[16] The following tests of memory and attention were selected according to the aims of the current study: selected tasks of the Alzheimer's Disease Assessment Scale–Cognitive 13-item subscale (ADAS-Cog 13),[22] including ADAS word list learning (immediate recall), ADAS word list recall (delayed recall), and ADAS figure learning, to assess verbal and spatial episodic memory. Attention was measured with the oral form of the Symbol-Digit-Modalities Test[23] and the Trail Making Test A and B[24] forms.

CSF biomarkers

Procedures for CSF acquisition, processing, and analysis in DELCODE have been previously described.[16] In the current study, we used the CSF Aβ42/Aβ40 ratio as a biomarker for amyloid-β pathology, CSF–phosphorylated tau181 levels as a biomarker for tau neurofibrillary tangles, and total CSF tau levels as a biomarker for unspecific neurodegeneration, according to the most recent NIA-AA guidelines AT(N) system.[6] The cut-off value for the Aβ42/Aβ40 ratio was < 0.09, based on a previous study[25]: cases below the cut-off of 0.09 were designated amyloid positive and cases above the cut-off as amyloid negative. CSF biomarkers were determined using

commercially available kits according to vendor specifications: V-PLEX Aβ Peptide Panel 1 (6E10) Kit (K15200E) and V-PLEX Human Total Tau Kit (K151LAE) (Mesoscale Diagnostics LLC, Rockville, USA), and Innotest Phospho-Tau(181P) (81581; Fujirebio Germany GmbH, Hannover, Germany).

CSF was sampled in those participants who consented to a lumbar punction (overall CSF sampling rate in DELCODE is around 50%). In the current study, we report the data for all participants with available CSF samples (n = 185, Supplementary Table 1). Participants with CSF samples did not differ from participants without CSF samples (n = 217) in key demographic variables and MMSE scores (Supplementary Table 2).

APOE genotyping

Genotypes for rs7412 and rs429358, the single nucleotide polymorphisms (SNPs) defining the ε-2, ε-3, and ε-4 alleles of *APOE*, were genotyped using the commercially available TaqMan® SNP Genotyping Assay (ThermoFisher Scientific). Both SNP assays were amplified on genomic DNA using a StepOnePlus Real-Time PCR System (ThermoFisher Scientific). Visual inspection of cluster formation was performed for each SNP before genotype data were used to define ε-2, ε-3, and ε-4 alleles in each sample. Participants were classified as *APOE*4 carriers if they were ε3/ε4 or ε4/ε4 carriers.

MRI Acquisition

The data were acquired from ten Siemens 3.0 Tesla MRI scanners using identical acquisition parameters and harmonised procedures. To ensure high image quality throughout the acquisition

phase, all scans had to pass a semiautomated quality check during the study conduction so that protocol deviations could be reported to the study sites, and the acquisition at the respective site could be adjusted.

High-resolution T1-weighted anatomical images were obtained using a sagittal magnetisation-prepared rapid gradient echo (MPRAGE) sequence (field of view 256 × 256 mm, matrix size 256 × 256, isotropic voxel size 1 mm, echo time 4.37 ms, flip angle 7°, repetition time 2500 ms, number of slices 192, parallel imaging acceleration factor 2).

An axial diffusion sequence was measured based on a single-shot echo planar imaging multi-shell sequence (field of view 240 × 240 mm, matrix size 120 × 120, isotropic voxel size 2 mm, repetition time 12100 ms, echo time 88 ms, flip angle 90°, number of slices 72, parallel imaging acceleration factor 2) with two diffusion-weighted shells at b = 700 s/mm^2 (30 volumes), and b = 1000 s/mm^2 (30 volumes). The sequence included 10 non-diffusion-weighted scans (b = 0 s/mm^2) evenly interspersed throughout the diffusion-weighted volumes.

A B0 field map was collected with matching geometry for use in unwarping EPI distortions due to magnetic field inhomogeneity.[26] The field map acquisition was performed with a 3D dual-echo spoiled gradient echo pulse sequence (field of view 240 x 240 mm, matrix size 80 x 80, isotropic voxel size 3 mm, number of slices 48, repetition time 675 ms, echo time 1 = 4.92 ms, echo time 2 = 7.38 ms, flip angle 60°).

Diffusion MRI-based modelling of the human cholinergic system

To characterise the microstructural properties of the human cholinergic system, a diffusion MRI-based in vivo model was derived. We followed the procedure described in a previous study.[27]

Briefly, the diffusion-weighted imaging data were preprocessed using FSL.[28] The non-brain tissue was removed,[29] EPI distortion was corrected using EPI-based field mapping,[30] and eddy currents and head motion were corrected.[31]

The estimation of the diffusion parameters in a standard ball-and-sticks model[32] for each voxel was performed with the graphics processing units accelerated version of the bedpostX toolbox,[33] considering three fibres modelled per voxel.

Next, two WM pathways originating from the NBM were captured, one traversing through the cingulum and one through the external capsule.[34] The NBM region of interest (ROI) was based on a cytoarchitectonic map of BF cholinergic nuclei in MNI space, derived from combined histology and *in cranio* MRI of a post-mortem brain.[35] The cingulum and external capsule masks were based on the Johns Hopkins University (JHU) WM atlas, available as part of the FSL package.[36]

Probabilistic tracking was performed by repeating 5000 random samples from each of the NBM ROI voxels and propagated through the local probability density functions of the estimated diffusion parameters.[37] Only the tracts traversing through the cingulum or external capsule ROI were kept.

Next, an unbiased template was created based on B0 pre-processed images from all HC cases using the Advanced Normalisation Tools (ANTs, http://stnava.github.io/ANTs/). After that, both pathways (through cingulum and external capsule) of all HC cases were non-linearly warped into the space of this unbiased template. Finally, pathway-specific binary masks were created by considering all the individual warped tracts and retaining only the voxels that were present (i.e.,

met by at least one fibre) in at least 60% of the cases. The 60% group threshold was chosen by visual inspection so that the resulting pathways were extensive yet still specific.

Extraction of diffusion indices

To characterise the microstructure properties of the tracked cholinergic pathways, we extracted the widely used indices of mean diffusivity (MD) and fraction anisotropy (FA) from the diffusion tensor model.

We calculated an average value of MD and FA indices for each participant and pathway, i.e., an average value of the diffusion index map within the cingulum and external capsule binary masks.

As a control, the remaining WM mask was created by excluding the two cholinergic WM pathways described above (i.e., a union of external capsule and cingulum pathways) from the whole WM mask. Then, we extracted the average values of MD and FA indices within the remaining WM mask using the same procedure.

We favoured the MD index to the FA index for its reduced susceptibility to the crossing-fibre problem. Nonetheless, we report FA results in the global analysis for reference.

NBM and hippocampal volumes

To evaluate the cell body damage of the cholinergic neurons, the NBM volume was estimated from the T1-weighted MR images. First, all the images were skull-stripped[29] and corrected for bias field.[38] Then, a non-linear spatial transformation to the MNI space where the NBM ROI resides was derived using ANTs. Finally, an individual NBM volume was calculated as the number of gray matter (GM) voxels with the back-transformed NBM ROI in native T1-weighted

space. The GM segmentation was obtained from the FSL's Automated Segmentation Tool (FAST).[38] The final NBM volume was adjusted by partial volume information provided by FAST. The total intracranial volume (TIV) was estimated based on the affine transformation in the FreeSurfer 6.0 image analysis suite (http://surfer.nmr.mgh.harvard.edu/). FreeSurfer was also used to segment the hippocampus (bilateral). Both the NBM and hippocampal volumes were normalised by the TIV to account for between-subject variability in head size.[39]

WM hypointensities

Previous studies have shown that the amount of small vessel disease (SVD) influences the integrity of the cholinergic WM pathways.[27,40] Hence, we included information about SVD status by means of WH-hypointensities. WM-hypointensities on T1-weighted images strongly correlate with WM hyperintensities as seen on T2/FLAIR images,[41] and with microstructural WM changes as measured on diffusion tensor imaging data.[42] Segmentation of WM-hypointensities and corresponding volumetrics was performed on T1-weighted images using the probabilistic procedure implemented in FreeSurfer 6.0.[43]

Statistical Analysis

Statistical analysis was carried out using the R programming language (The R Foundation for Statistical Computing; version 4.0.3). Results were deemed statistically significant at two-tailed $p < 0.05$.

Demographics

Demographics were group-wise compared between HC and all other diagnostic groups using independent *t*-tests for age and years of education, and Chi-square tests for sex and *APOE* genotype. Differences in cognitive measures and CSF biomarkers between diagnostic groups were compared using a one-way analysis of variance with covariates (ANCOVA) with age and sex as covariates. ANCOVA was followed by paired *post hoc t*-tests adjusting for multiple comparisons with the Tukey method. Our comparisons of interest were SCD vs. HC, MCI vs. HC, and AD dementia vs. HC. The extracted NBM and hippocampus volumes corrected for the TIV, and WM-hypointensities load were also compared using ANCOVA, controlling for age and sex.

Pathway integrity comparison (global and voxel-wise)

To assess the differences in the integrity of the tracked pathways between groups, we ran analysis both in aggregated (average, as a global measure) and voxel-wise manner. Firstly, we analysed group-wise differences of the FA and MD averages in the cingulum, external capsule, and remaining WM control mask using analyses of covariance (ANCOVA) with age and sex as covariates. ANCOVA was followed by paired *post hoc t*-tests adjusting for multiple comparisons with the Tukey method. Our comparisons of interest were SCD vs. HC, MCI vs. HC, and AD dementia vs. HC. However, we also report the results for the remaining pairs for the sake of completeness (SCD vs. MCI, SCD vs. AD dementia, and MCI vs. AD dementia). Next, to assess the more detailed spatial differences in the integrity of the pathways, we applied a voxel-wise generalised linear model (GLM) using permutation-based non-parametric testing (randomise),[44] and correcting for multiple comparisons across space (threshold-free cluster enhancement,

TFCE), with age and sex as covariates. For this, we previously warped all individual MD maps into a common space of the unbiased template using non-linear warp field originated from registering respective individual B0 images to the unbiased template. Significance maps were corrected for multiple comparisons using a familywise error rate of $p < 0.05$. To assess the association between CSF biomarkers of AD-related pathology and integrity in cholinergic WM pathways, we performed Pearson correlations.

Importance analysis using random forest

To assess the association of MRI markers of the cholinergic system with cognitive performance, we conducted several random forest (RF) analyses with cognitive performance as outcome variables and MD in the cingulum WM pathway, MD in the external capsule WM pathway, and NBM volume as predictors. We also included MD in the remaining WM as a negative control for the cholinergic WM. Further, we included WM-hypointensities as an extra predictor because our clinical groups differed in WM hypointensity load, and we had previously demonstrated that WM hypointensities make a major contribution to integrity in cholinergic WM pathways.[27,45] Finally, we also included age, sex and years of education to consider the contribution of these variables, as they usually influence cognitive performance. To compare the role of the integrity of the cholinergic pathways and the NBM volume along the AD continuum, we created two separate RF models, one for HC and SCD combined and one for MCI and AD combined. We combined the groups to gain sufficient statistical power, keeping separated RF models for groups with normal cognition (HC and SCD) and groups with impaired cognition (MCI and AD dementia).

We used RF regression with a conditional inference tree for unbiased variable selection. RF is an ensemble method in machine learning that involves growing multiple decision trees via bootstrap aggregation (bagging). Each tree predicts a classification independently and votes for the corresponding class. The majority of the votes decides the overall prediction.[46,47] RF has important advantages over other regression techniques in terms of ability to handle highly non-linear biological data, robustness to noise, and tuning simplicity.[48]

Conditional feature importance scores for random forest were computed by measuring the increase in prediction error if the values of a variable under question are permuted within a grid defined by the covariates that are associated with the variable of interest. This score is computed for each constituent tree and averaged across the entire ensemble. The conditional feature importance scores were designed to diminish an undesirable effect of preference of correlated predictor variables. Variables receiving higher importance scores are more likely to be closely linked to the output variable (cognitive scores). The RF was comprised of 2000 conditional inference trees. The *party* package[49] was used for this analysis.

Biomarker discriminative power (ROC analysis)

To investigate the capacity of the suggested biomarkers (integrity of all considered pathways and BF and hippocampus volumes) to discriminate the different clinical groups from the HC group, the receiver operating characteristic (ROC) curve analysis was carried out. The analysis was performed each time between the HC group and one of the clinical groups, resulting in three different performance models (one for SCD, one for MCI, and one for AD dementia subjects). Next, we computed the area under the ROC curve (AUC) for each curve as a cumulative statistic

of the overall discriminative power of the biomarker in question. AUCs were then pair-wise compared using the bootstrap method (2000 replications) from the *pROC* package.[50]

Data availability

Requests for access to the data and code used in this study should be directed to the corresponding author. Our data sharing complies with the requirements of our funders and institutes, as well as with institutional ethics approval.

Results

Demographic characteristics, cognitive performance, and MRI and CSF biomarkers across study groups

Demographic data are shown in Table 1. All clinical groups (SCD, MCI, AD dementia) were significantly older than the HC group ($p_{SCD} = 0.005$, $p_{MCI} < 0.001$, $p_{AD} < 0.001$). The SCD and MCI groups had a higher frequency of men than the HC group ($p_{SCD} = 0.033$, $p_{MCI} = 0.004$). The AD dementia group had significantly fewer years of education ($p_{AD} < 0.001$) and together with the MCI group showed worse performance in the MMSE than the HC group ($p_{MCI} < 0.001$, $p_{AD} < 0.001$). MCI and AD dementia groups (but not SCD) performed worse than the HC group in ADAS word list learning (immediate recall) ($p_{MCI} < 0.001$, $p_{AD} < 0.001$), ADAS figure learning (recall) ($p_{MCI} < 0.001$, $p_{AD} < 0.001$), Trail making test A ($p_{MCI} = 0.043$, $p_{AD} < 0.001$), Trail making test B ($p_{MCI} < 0.001$, $p_{AD} < 0.001$), and symbol digit modalities ($p_{MCI} < 0.001$, $p_{AD} < 0.001$). There were differences in ADAS word list learning (delayed recall) in all diagnostic groups when compared with the HC group ($p_{SCD} = 0.043$, $p_{MCI} < 0.001$, $p_{AD} < 0.001$).

NBM and hippocampal volumes were significantly lower in all clinical groups as compared with the HC group (NBM volume: $p_{SCD} = 0.049$, $p_{MCI} < 0.001$, $p_{AD} < 0.001$, hippocampal volume: $p_{SCD} = 0.018$, $p_{MCI} < 0.001$, $p_{AD} < 0.001$), with age and sex adjusted in the model. WM-hypointensity volume was significantly higher only in MCI and AD dementia groups as compared with the HC group ($p_{MCI} = 0.031$, $p_{AD} < 0.001$), with age and sex adjusted in the model. The frequency of *APOE*4 carriers was significantly higher only in the MCI and AD groups in comparison to the HC group ($p_{MCI} < 0.001$, $p_{AD} < 0.001$). Qualitative inspection shows that 31% of the SCD individuals were APOE4 carriers, while only 22% of the HC individuals were APOE4 carriers.

The subset with available CSF biomarkers ($N = 185$, 46% of the total sample) showed no significant differences between SCD and HC groups in any of the CSF biomarkers. On the other hand, MCI and AD dementia groups showed a significant decrease in the Aβ42/Aβ40 ratio, and a significant increase in total tau and p-tau181 levels (Aβ42/Aβ40 ratio: $p_{MCI} < 0.001$, $p_{AD} < 0.001$, total tau: $p_{MCI} = 0.035$, $p_{AD} < 0.001$, p-tau181: $p_{MCI} = 0.044$, $p_{AD} < 0.001$), as compared with the HC group. Moreover, MCI and AD dementia groups also showed a significant decrease in the Aβ42/Aβ40 ratio, and a significant increase in total tau and p-tau181 levels ($p < 0.001$ in all comparisons), as compared with the SCD group. All CSF biomarker analyses included age and sex as covariates.

Integrity of cholinergic pathways along the AD continuum: global analysis

Fig. 1 and Supplementary Table 6 show the average FA and MD values of the tracked pathways along the AD continuum, with all analyses controlled for age and sex. We observed a significant

average decrease of FA and an average increase of MD in SCD individuals as compared with the HC group ($p < 0.001$ in all comparisons, for both pathways), demonstrating early alterations of cholinergic pathways in the AD continuum.

The same differences in FA and MD average measures were observed in the MCI and AD dementia groups compared to the HC group ($p < 0.001$ in all comparisons, for both pathways). In the remaining WM, only the average FA values in MCI and AD, and the average MD values in SCD and AD showed significant differences when compared to the HC group (average FA: $p_{MCI} = 0.002$, $p_{AD} < 0.001$, average MD: $p_{SCD} = 0.020$, $p_{AD} < 0.001$).

In the amyloid stratified subsample, we observed a similar pattern of findings in both cholinergic pathways (Supplementary Fig. 1). In contrast with the whole sample, the group differences in the remaining WM in SCD and MCI groups when compared to the HC group were non-significant.

All pair-wise post hoc statistics are summarised in Supplementary Table 3 and Supplementary Table 4.

Lastly, we observed a statistically significant correlation between integrity of cholinergic WM pathways with CSF biomarkers of AD pathology: MD in cingulum pathway and A42/40: $r_{(183)} = -0.221$, $p < 0.01$; MD in external capsule pathway and Aβ42/40: $r_{(183)} = -0.248$, $p < 0.001$; MD in cingulum pathway and p-tau: $r_{(183)} = 0.169$, $p < 0.05$; MD in external capsule pathway and p-tau: $r_{(183)} = 0.199$, $p < 0.01$; MD in cingulum pathway and total tau: $r_{(183)} = 0.198$, $p < 0.01$; and MD in external capsule pathway and total tau: $r_{(183)} = 0.247$, $p < 0.001$.

Integrity of cholinergic pathways along the AD continuum: regional (voxel-wise) analysis

Fig. 2 and Fig. 3 show statistical maps of voxel-wise differences in MD between groups, in cingulum and external capsule pathways. All analyses were controlled for age and sex.

The cingulum pathway (Fig. 2) showed significantly higher MD values in the retrosplenial and posterior cingulate already in the SCD group when compared with the HC, suggesting an early regional vulnerability of posterior cholinergic WM in the AD continuum.

In the MCI group, these differences were spatially more pronounced and complemented by significant differences in a small area in the rostral anterior cingulate. In the AD dementia group, all the differences visible in the MCI group were present, but further spatially extended and were statistically more pronounced, with additional significant differences in the dorsal anterior cingulate. Differences in MD values in the WM underneath NBM emerged only in the MCI and AD dementia groups, but not in the SCD group, when compared with the HC group. This could suggest that it is distal cholinergic WM what shows the earliest alterations in the AD continuum.

The external capsule pathway (Fig. 3) showed a resembling pattern of differences in MD values in the SCD and MCI groups: in the external capsule, retrosplenial and posterior cingulate, and parts of the uncinate fasciculus. In the AD dementia group, there were noticeable additional differences in temporal and prefrontal WM areas when compared with the HC group. Hence, again, these findings suggest an early regional vulnerability of posterior cholinergic WM in the AD continuum.

The same overall pattern of results could be observed when we repeated the voxel-wise analysis in the amyloid stratified subsample (Supplementary Fig. 2 and Supplementary Fig. 3). Despite

the reduced statistical power, we again observed significant differences already in the SCD group, both in cingulum and external capsule pathways, which became more prominent in the MCI and AD groups.

Contribution of the integrity of cholinergic pathways to cognitive performance

Fig. 4 shows the degree of contribution of MD in cingulum and external capsule pathways, MD in remaining WM, WM-hypointensities, and NBM volume towards cognitive measures of memory and attention, as examined by random forest analysis. Additional independent variables were age, sex, and years of education. These analyses were conducted separately for the groups with normal cognition (HC and SCD) and the groups with impaired cognition (MCI and AD dementia). Independent variables in each plot in Fig. 4 are presented in descending order of their importance score.

In the normal cognition groups (HC and SCD), sex, age, and years of education were among the most important variables in the prediction of ADAS memory tests. MD in the external capsule pathway had a stronger importance in attention tests (Symbol digit modalities test, and Trail making test B). NBM volume and WM-hypointensities received low importance scores in all the random forest models. Scores from the Trail making test A failed to be predicted by the respective random forest model.

In the impaired cognition groups (MCI and AD dementia), NBM volume was among the most important predictors for ADAS word list learning and recall, Symbol digit modalities test and Trail making test B. MD in the external capsule pathway was important towards all ADAS

memory tests and Trail making test A. MD in the cingulum pathway was a noticeable contributor only in the prediction of Trail making test A. WM-hypointensities and MD in the remaining WM received low importance scores in all the random forest models.

In summary, particularly the integrity of the external capsule pathway contributed to predict performance in attention tests in HC and SCD individuals. The contribution of cholinergic pathways (and NBM volume) to cognitive performance became stronger in the MCI and AD dementia groups, both for memory and attention tests, and also including the cingulum pathway.

Integrity of cholinergic pathways discriminate the SCD group better than conventional volumetric measures (ROC analysis)

The ROC curves and their corresponding AUCs indicated how well each of the considered biomarkers can be used to distinguish between a clinical group and the HC group. Please see Fig. 5 for *p*-values and Supplementary Table 5 for AUC values.

MD in the external capsule (ExCap) (AUC_{ExCap} = 0.736) performed significantly better than all the other biomarkers in distinguishing SCD from HC. The second-best performing biomarker was MD in the cingulum (Cing) (AUC_{Cing} = 0.713). AUCs of MD in the remaining WM (rem), NBM volume, and hippocampus volume had the lowest discriminative performance and were not significantly different from each other: AUC_{MD_rem} = 0.663, AUC_{NBM_vol} = 0.625, AUC_{hipp_vol} = 0.660.

In the case of MCI, all biomarkers except for MD (rem. WM) reached statistically comparable high AUC values: AUC_{NBM_vol} = 0.792, AUC_{hipp_vol} = 0.845, AUC_{MD_Cing} = 0.813, AUC_{MD_ExCap} =

0.833. In contrast, MD (rem. WM) performed significantly poorer than all the other biomarkers (AUC_{MD_rem} = 0.676).

For the AD dementia group, hippocampus volume, NBM volume, and MD (Ex. cap.) performed equally high: AUC_{hipp_vol} = 0.936, AUC_{NBM_vol} = 0.936, AUC_{MD_ExCap} = 0.901. *P*-values showed that MD (Cing) (AUC_{Cing} = 0.869) showed slightly worse performance than hippocampus volume and MD (ExCap), and MD (rem. WM) had the worst value (AUC_{MD_rem} = 0.745).

In summary, the results of the ROC analysis were stage specific. Cholinergic WM pathways outperformed other biomarkers in the SCD group. Generally, all the considered biomarkers performed better with a more advanced clinical stage of the disease in the AD continuum.

The findings were very similar in the amyloid stratified subsample (Supplementary Fig. 4, Supplementary Table 4). In the amyloid-positive SCD cases, the NBM volume performed worse than all the other biomarkers. In the amyloid-positive MCI cases, MD (Cing), MD (ExCap) and hippocampus volume were better than NBM volume and MD (rem. WM). In the amyloid-positive AD dementia cases, all biomarkers performed better than MD (rem. WM).

Discussion

We investigated DTI-based integrity of the human cholinergic system along the AD continuum, including SCD individuals as a group reflecting the preclinical stage of AD (particularly amyloid-positive SCD individuals). The study focused on the integrity of the cholinergic WM pathways, including differences between clinical stages, their predictive power compared to conventional volumetric MRI biomarkers, and their association to cognitive performance. We found reduced integrity of the cholinergic pathways in all the stages of the AD continuum (SCD,

MCI, and AD dementia). The spatial distribution of these differences followed a posterior-anterior pattern. Differences in the SCD stage involved posterior cholinergic WM and, at more advanced stages, we also found differences in anterior frontal WM. All considered biomarkers (conventional volumetric and novel measures of WM integrity) showed higher predictive power at more advanced stages within the AD continuum. However, measures of the integrity of the cholinergic pathways were more informative in distinguishing SCD from HC than all other biomarkers. The multivariate models showed that the integrity of the cholinergic pathways and NBM volume, but not the integrity of the rest of WM, strongly contributed to performance in attention and memory in cognitively impaired individuals (MCI and AD dementia).

In the whole sample, we found that the integrity of the cholinergic WM pathways was reduced in all stages of the AD continuum. The findings for the MCI and AD dementia groups thus agree with a recent study that showed that NBM degeneration is accompanied by alterations of cholinergic WM pathways in MCI and AD dementia.[14] Additionally, a recent post-mortem study based on post-mortem MRI and histopathology reported no significant differences between AD and HC in cholinergic WM pathways, but demonstrated that decreased cholinergic cell density in NBM was associated with reduced integrity of cholinergic WM pathways towards the temporal lobe.[51] Our current study extends these previous studies by showing that the integrity of cholinergic pathways is already altered at the stage of SCD.

We did not observe any statistically significant differences in CSF biomarkers between the SCD and HC groups. These results are in line with previous studies that showed no significant differences in CSF biomarkers in SCD compared to HC.[52–55] There are however some reports about significant differences in CSF biomarkers between SCD and HC groups.[56] These differences have also been observed in CSF and PET AD biomarkers in SCD individuals who

progressed to MCI or dementia.[57,58] The observed lack of statistical differences in our study and by others could mean that degeneration of the cholinergic system may precede measurable changes in conventional biomarkers for AD pathology (amyloid-β and tau biomarkers). A similar conclusion has been made by a study of basal forebrain volume.[59] Alternatively, perhaps more sensitive CSF biomarkers such as N-224 could detect AD pathology in the absence of statistical differences for Aβ42/Aβ40 ratio and p-tau181 CSF biomarkers.[56,60]

The reduced integrity of the cholinergic pathways in all stages of the AD continuum was replicated in the amyloid stratified subsample, thus supporting our findings both in clinically and biologically defined study groups. In addition, the integrity of the remaining WM was reduced in all stages of the continuum, in the whole sample. This global WM degeneration has also been reported by others.[61] However, this reduction of integrity of remaining WM could not be clearly observed in the amyloid stratified subsample. Although this could be explained by the small sample size, the integrity of both cholinergic pathways remained significantly different between clinical groups and HC in the amyloid stratified subsample, hence, with the same sample size. This could possibly mean that while the remaining WM deteriorates and its changes in integrity provide information about the global degeneration, the considered cholinergic pathways and their integrity are particularly sensitive to an Alzheimer's pathologic change (amyloid-β positivity). This hypothesis could be further supported by our statistically significant correlation between CSF amyloid-β levels and integrity of cingulum and external capsule pathways. In addition, we also showed a statistically significant correlation between CSF tau biomarkers and integrity of cingulum and external capsule pathways, supporting the association between cholinergic WM and AD-related pathology. Although there are no studies investigating in vivo cholinergic projections in AD other than the recent study by Schumacher et al.[14], studies focusing on NBM

volume similarly reported that NBM volume is more closely associated with AD-related pathology than other GM areas.[59,62] This finding is also supported by our ROC analysis, in which the integrity of remaining WM performed consistently poorer in all cases.

Another finding this study provides is the spatial distribution of differences in WM integrity of the cholinergic pathways, along the AD continuum. We demonstrated that the SCD group already showed a clear pattern of reduced integrity in the retrosplenial and posterior cingulate cortex, as well as in the external capsule. These regions were previously identified as the ones with the earliest neuronal and metabolic changes and reduced connectivity, emerging as a vulnerable AD-associated epicenter.[63] Also, these regions have been associated with early accumulation of amyloid in PET studies.[64] Differences in the MCI group included the same areas as in the SCD group and, additionally, involved the rostral anterior cingulate. In AD dementia, WM integrity alterations extended to the dorsal anterior cingulate and temporal and prefrontal areas. These areas are usually associated with increased neuronal loss in MCI and AD dementia,[65] but here we show involvement of the cholinergic WM. Despite the cross-sectional nature of our analyses, the replication of regional damage as the disease progresses, as well as the stepwise addition of cholinergic WM areas following a posterior-anterior pattern of degeneration is a robust finding. If replicated in longitudinal designs, these findings could help understanding the progression of cholinergic system changes in vivo, along the development of AD.

Finally, random forest analysis showed a substantially different set of important predictors of cognitive scores in cognitively unimpaired and impaired groups. In the analysis of HC and SCD groups combined, it was mainly age, sex, and years of education that counted towards the cognitive performance. On top of that, the integrity of the external capsule pathway played a

moderately important role in tests of attention. The external capsule pathway projects to cortices involved in attention such as regions located in frontal lobe and posterior cortex. On the other hand, in the analysis involving cognitively impaired groups (MCI and AD dementia), integrity in the external capsule and cingulum pathways was important towards most of the tests of memory and attention. In addition to frontal and posterior cortical areas, the external capsule pathway also projects to cortices related to memory such as medial temporal structures. The cingulum pathway also projects to cortices related to memory such as hippocampal structures and posterior cingulate cortex. These findings reflect the role of cholinergic system in cognitive process of effortful attention and memory. Integrity in the remaining WM was not important. Similar results have recently been reported in studies conducted in healthy aging[27] and in AD and dementia with Lewy bodies.[14,51] In our cognitively unimpaired groups (HC and SCD), we could practically replicate the results in Nemy et al.[27] which were based on independent data. Firstly, we observed that age and sex were important variables towards the prediction of most of the cognitive tests. Secondly, the integrity of cholinergic pathways received considerably high importance score only towards tests involving effortful attention. The difference in average age of 15 years between our current cohort and the participants in Nemy et al.[27] suggests that these findings may be generalizable across age groups. In addition, in the current study we observed that NBM volume was important towards performance in memory and attention tests in the MCI and AD dementia groups. This is in line with other studies investigating AD[66] and Parkinson's disease,[67] which found that NBM volume is an important predictor of disease progression. Altogether, these findings suggest that the cholinergic system may deteriorate earlier in the WM, and NBM volume would follow in more advanced stages of the disease. In keeping with the posterior-anterior pattern of WM cholinergic disruption, this observation might suggest that NBM starts

deteriorating when enough cholinergic WM damage has occurred. This dying-back pattern of degeneration known as 'Wallerian-like degeneration' has been demonstrated in AD in several experimental and pathological studies.[11,68] All in all, these results illustrate the early involvement of cholinergic pathways in the AD continuum and add additional evidence that the employed methodology using DTI tracking is a promising and emerging potential biomarker of microstructural changes within earliest stages of AD.

All the findings discussed above are further underlined by the results of our ROC analysis. Firstly, all considered biomarkers, both conventional volumetric and novel measures of WM integrity, showed higher predictive importance with the progression of the disease. This finding validates the conventional volumetric biomarkers but also suggests that the proposed measures of WM integrity are sensitive to neurodegeneration changes along the AD continuum. Consistent low predictive power of remaining WM integrity in ROC analysis points out that the measures of the cholinergic system pathways are not only sensitive but also specific. Secondly, the ROC data showed significantly better predictive power of integrity of cholinergic WM pathways than the conventional volumetric measures in the SCD group. This might suggest that the proposed cholinergic biomarkers are more suitable for detecting very early changes in the disease. Thirdly, whereas in the whole sample the predictive power of the NBM volume appeared approximately on the same level as the integrity of at least one of the cholinergic WM pathways, in the amyloid-positive subsample the NBM volume performed significantly worse than both cholinergic WM pathways in distinguishing SCD and MCI from HC. This further supports the hypothesis that alterations of cholinergic WM projections occur earlier than neurodegeneration in NBM, in the context of an Alzheimer's pathologic change (amyloid-β positivity).

This study has some limitations. We primarily aimed to investigate cross-sectional differences along the AD continuum and interpretations about cholinergic WM pathways and clinical progression were based on different groups. Whereas this approach serves as a preliminary demonstration of early differences in cholinergic WM pathways in the SCD group, that extends to other WM areas in the MCI and AD dementia groups, it will be important to expand our current approach to include longitudinal analyses in the future. Longitudinal analyses will be needed to confirm our preliminary interpretation of cholinergic alterations preceding AD pathology (positivity both in amyloid-β and tau biomarkers). Next, CSF biomarkers were not available for all subjects in the cohort. Although the CSF biomarker subsample was large enough to allow for replication of the main results, the analysis would benefit from having an even larger CSF sample. Our comparison of participants with and without CSF data available did not show any difference in terms of key demographic variables and MMSE scores, suggesting a low risk for selection bias with regards the subsample with CSF data available. Furthermore, even with standardised MRI acquisition protocols and careful image quality control, we cannot completely exclude that inter-scanner variance may have influenced some of our results.[69] However, since the focus of this study mostly involved comparison of within-subject measures (i.e., conventional volumetric vs cholinergic WM integrity biomarkers), our main conclusions should not be affected by inter-scanner variance. We also provide the break down of study participants by scanner in Supplementary Table 7, for the reader's interest. Lastly, voxel-wise analysis showed significant differences in MD in posterior parts of the cholinergic pathways between SCD and HC. However, when using an average measure of MD in the entire cholinergic pathways, we did not observe a pronounced contribution of the cholinergic pathways to cognition in the random

forest models. Future studies could explore the contribution of more regional measures of MD to cognitive performance in SCD individuals.

In conclusion, we modelled in vivo cholinergic WM pathways and investigated their integrity along the stages of the AD continuum, and in relation to cognitive performance. We showed that the integrity of the cholinergic WM pathways is associated to AD-related pathology, and it reveals alterations as early as the stage of SCD. The cholinergic WM pathways differentiated between SCD and HC groups better than the integrity of non-cholinergic WM and conventional measures of hippocampal and NBM volumes. These findings suggest that the integrity of WM cholinergic pathways is a sensitive and specific biomarker of early neurodegeneration in individuals with an Alzheimer's pathologic change (amyloid-β positivity).

Funding

This study was supported by the Swedish Research Council (2020-02014); the regional agreement on medical training and clinical research (ALF) between Stockholm County Council and Karolinska Institutet; Center for Innovative Medicine (CIMED); the Swedish Alzheimer Foundation; the Swedish Brain Foundation; Neuro Fonden, the Czech Alzheimer Foundation; and Demensfonden. Research of M.N., O.S. and L.V. was partially supported by institutional resources of Czech Technical University in Prague. The work was further supported by a grant to S.J.T. within the CureDem funding of the Federal Ministry of Research (BMBF), grant number 01KX2130. The funding sources did not have any involvement in the study design; collection, analysis, and interpretation of data; writing of the report; and the decision to submit the article for publication.

Competing interests

S.J.T. participated in scientific advisory boards of Roche Pharma AG, Biogen, GRIFOLS, EISAI, and MSD, and received lecture fees from Roche and MSD. M.N., O.S., L.V., and D.F. report no competing interests.

Supplementary material

Supplementary material is available at *Brain* online.

References

1. Buchhave P, Minthon L, Zetterberg H, Wallin ÅK, Blennow K, Hansson O. Cerebrospinal fluid levels of β-amyloid 1-42, but not of tau, are fully changed already 5 to 10 years before the onset of Alzheimer dementia. *Arch Gen Psychiatry*. 2012;69(1):98-106. doi:10.1001/archgenpsychiatry.2011.155
2. Villemagne VL, Burnham S, Bourgeat P, et al. Amyloid β deposition, neurodegeneration, and cognitive decline in sporadic Alzheimer's disease: A prospective cohort study. *Lancet Neurol*. 2013;12(4):357-367. doi:10.1016/S1474-4422(13)70044-9
3. Albert M, Zhu Y, Moghekar A, et al. Predicting progression from normal cognition to mild cognitive impairment for individuals at 5 years. *Brain*. 2018;141(3):877-887. doi:10.1093/brain/awx365
4. Sperling RA, Aisen PS, Beckett LA, et al. Toward defining the preclinical stages of Alzheimer's disease: Recommendations from the National Institute on Aging-Alzheimer's Association workgroups on diagnostic guidelines for Alzheimer's disease. *Alzheimer's Dement*. 2011;7(3):280-292. doi:10.1016/j.jalz.2011.03.003
5. Dubois B, Hampel H, Feldman HH, et al. Preclinical Alzheimer's disease: Definition, natural history, and diagnostic criteria. *Alzheimer's Dement*. 2016;12(3):292-323. doi:10.1016/j.jalz.2016.02.002
6. Jack CR, Bennett DA, Blennow K, et al. NIA-AA Research Framework: Toward a

biological definition of Alzheimer's disease. *Alzheimer's Dement*. 2018;14(4):535-562. doi:10.1016/j.jalz.2018.02.018

7. Fu H, Hardy J, Duff KE. Selective vulnerability in neurodegenerative diseases. *Nat Neurosci*. 2018;21(10):1350-1358. doi:10.1038/s41593-018-0221-2

8. Brueggen K, Dyrba M, Barkhof F, et al. Basal forebrain and hippocampus as predictors of conversion to Alzheimer's disease in patients with mild cognitive impairment-a multicenter DTI and volumetry study. *J Alzheimer's Dis*. 2015;48(1):197-204. doi:10.3233/JAD-150063

9. Schmitz TW, Nathan Spreng R, Initiative TADN, et al. Basal forebrain degeneration precedes and predicts the cortical spread of Alzheimer's pathology. *Nat Commun*. 2016;7(1):13249. doi:10.1038/ncomms13249

10. Bartus RT, Dean RL, Beer B, Lippa AS. The cholinergic hypothesis of geriatric memory dysfunction. *Science*. 1982;217(4558):408-414. doi:10.1126/SCIENCE.7046051

11. Kanaan NM, Pigino GF, Brady ST, Lazarov O, Binder LI, Morfini GA. Axonal degeneration in Alzheimer's disease: When signaling abnormalities meet the axonal transport system. *Exp Neurol*. 2013;246:44-53. doi:10.1016/j.expneurol.2012.06.003

12. Li X, Li TQ, Andreasen N, Wiberg MK, Westman E, Wahlund LO. The association between biomarkers in cerebrospinal fluid and structural changes in the brain in patients with Alzheimer's disease. *J Intern Med*. 2014;275(4):418-427. doi:10.1111/joim.12164

13. Li X, Westman E, Ståhlbom AK, et al. White matter changes in familial Alzheimer's disease. *J Intern Med*. 2015;278(2):211-218. doi:10.1111/joim.12352

14. Schumacher J, Ray NJ, Hamilton CA, et al. Cholinergic white matter pathways in dementia with Lewy bodies and Alzheimer's disease. *Brain*. Published online October 4, 2021. doi:10.1093/brain/awab372

15. Ballinger EC, Ananth M, Talmage DA, Role LW. Basal Forebrain Cholinergic Circuits and Signaling in Cognition and Cognitive Decline. *Neuron*. 2016;91(6):1199-1218. doi:10.1016/j.neuron.2016.09.006

16. Jessen F, Spottke A, Boecker H, et al. Design and first baseline data of the DZNE multicenter observational study on predementia Alzheimer's disease (DELCODE). *Alzheimer's Res Ther*. 2018;10(1):21. doi:10.1186/s13195-017-0314-2

17. Folstein MF, Folstein SE, McHugh PR. "Mini-mental state". A practical method for

grading the cognitive state of patients for the clinician. *J Psychiatr Res*. 1975;12(3):189-198. doi:10.1016/0022-3956(75)90026-6

18. Yesavage JA, Sheikh JI. Geriatric Depression Scale (GDS). *Clin Gerontol*. 1986;5(1-2):165-173. doi:10.1300/J018v05n01_09

19. Jessen F, Amariglio RE, Van Boxtel M, et al. A conceptual framework for research on subjective cognitive decline in preclinical Alzheimer's disease. *Alzheimer's Dement*. 2014;10(6):844-852. doi:10.1016/j.jalz.2014.01.001

20. Albert MS, DeKosky ST, Dickson D, et al. The diagnosis of mild cognitive impairment due to Alzheimer's disease: Recommendations from the National Institute on Aging-Alzheimer's Association workgroups on diagnostic guidelines for Alzheimer's disease. *Alzheimer's Dement*. 2011;7(3):270-279. doi:10.1016/j.jalz.2011.03.008

21. McKhann GM, Knopman DS, Chertkow H, et al. The diagnosis of dementia due to Alzheimer's disease: Recommendations from the National Institute on Aging-Alzheimer's Association workgroups on diagnostic guidelines for Alzheimer's disease. *Alzheimer's Dement*. 2011;7(3):263-269. doi:10.1016/j.jalz.2011.03.005

22. Mohs RC, Knopman D, Petersen RC, et al. Development of cognitive instruments for use in clinical trials of antidementia drugs: Additions to the Alzheimer's disease assessment scale that broaden its scope. *Alzheimer Dis Assoc Disord*. 1997;11(SUPPL. 2). doi:10.1097/00002093-199700112-00003

23. Smith A. Symbol digit modality test (SDMT): manual (revised). *Psychol Serv Los Angeles*. Published online 1982.

24. Reitan RM. Validity of the Trail Making Test as an Indicator of Organic Brain Damage. *Percept Mot Skills*. 1958;8(3):271-276. doi:10.2466/pms.1958.8.3.271

25. Janelidze S, Zetterberg H, Mattsson N, et al. CSF Aβ42/Aβ40 and Aβ42/Aβ38 ratios: Better diagnostic markers of Alzheimer disease. *Ann Clin Transl Neurol*. 2016;3(3):154-165. doi:10.1002/acn3.274

26. Jezzard P, Balaban RS. Correction for geometric distortion in echo planar images from B0 field variations. *Magn Reson Med*. 1995;34(1):65-73. doi:10.1002/mrm.1910340111

27. Nemy M, Cedres N, Grothe MJ, et al. Cholinergic white matter pathways make a stronger contribution to attention and memory in normal aging than cerebrovascular health and nucleus basalis of Meynert. *Neuroimage*. 2020;211:116607.

doi:10.1016/j.neuroimage.2020.116607

28. Jenkinson M, Beckmann CF, Behrens TEJ, Woolrich MW, Smith SM. FSL. *Neuroimage*. 2012;62(2):782-790. doi:10.1016/j.neuroimage.2011.09.015

29. Smith SM. Fast robust automated brain extraction. *Hum Brain Mapp*. 2002;17(3):143-155. doi:10.1002/hbm.10062

30. Reber PJ, Wong EC, Buxton RB, Frank LR. Correction of off resonance-related distortion in echo-planar imaging using EPI-based field maps. *Magn Reson Med*. 1998;39(2):328-330. doi:10.1002/mrm.1910390223

31. Andersson JLR, Sotiropoulos SN. An integrated approach to correction for off-resonance effects and subject movement in diffusion MR imaging. *Neuroimage*. 2016;125:1063-1078. doi:10.1016/j.neuroimage.2015.10.019

32. Behrens TEJ, Berg HJ, Jbabdi S, Rushworth MFS, Woolrich MW. Probabilistic diffusion tractography with multiple fibre orientations: What can we gain? *Neuroimage*. 2007;34(1):144-155. doi:10.1016/j.neuroimage.2006.09.018

33. Hernández M, Guerrero GD, Cecilia JM, et al. Accelerating Fibre Orientation Estimation from Diffusion Weighted Magnetic Resonance Imaging Using GPUs. *PLoS One*. 2013;8(4). doi:10.1371/journal.pone.0061892

34. Selden NR, Gitelman DR, Salamon-Murayama N, Parrish TB, Mesulam MM. Trajectories of cholinergic pathways within the cerebral hemispheres of the human brain. *Brain a J Neurol*. 1998;121(12):2249-2257. doi:10.1093/brain/121.12.2249

35. Kilimann I, Grothe M, Heinsen H, et al. Subregional basal forebrain atrophy in alzheimer's disease: A multicenter study. *J Alzheimer's Dis*. 2014;40(3):687-700. doi:10.3233/JAD-132345

36. Mori S, Wakana S, Van Zijl PC, Nagae-Poetscher L. *MRI Atlas of Human White Matter*. Elsevier; 2005.

37. Behrens TEJ, Woolrich MW, Jenkinson M, et al. Characterization and Propagation of Uncertainty in Diffusion-Weighted MR Imaging. *Magn Reson Med*. 2003;50(5):1077-1088. doi:10.1002/mrm.10609

38. Zhang Y, Brady M, Smith S. Segmentation of brain MR images through a hidden Markov random field model and the expectation-maximization algorithm. *IEEE Trans Med Imaging*. 2001;20(1):45-57. doi:10.1109/42.906424

39. Buckner RL, Head D, Parker J, et al. A unified approach for morphometric and functional data analysis in young, old, and demented adults using automated atlas-based head size normalization: Reliability and validation against manual measurement of total intracranial volume. *Neuroimage*. 2004;23(2):724-738. doi:10.1016/j.neuroimage.2004.06.018
40. Kim HJ, Moon WJ, Han SH. Differential cholinergic pathway involvement in alzheimer's disease and subcortical ischemic vascular dementia. *J Alzheimer's Dis*. 2013;35(1):129-136. doi:10.3233/JAD-122320
41. Cedres N, Ferreira D, Machado A, et al. Predicting Fazekas scores from automatic segmentations of white matter signal abnormalities. *Aging (Albany NY)*. 2020;12(1):894-901. doi:10.18632/aging.102662
42. Leritz EC, Shepel J, Williams VJ, et al. Associations between T1 white matter lesion volume and regional white matter microstructure in aging. *Hum Brain Mapp*. 2014;35(3):1085-1100. doi:10.1002/hbm.22236
43. Fischl B, Salat DH, Busa E, et al. Whole brain segmentation: automated labeling of neuroanatomical structures in the human brain. *Neuron*. 2002;33(3):341-355. doi:10.1016/S0896-6273(02)00569-X
44. Winkler AM, Ridgway GR, Webster MA, Smith SM, Nichols TE. Permutation inference for the general linear model. *Neuroimage*. 2014;92:381-397. doi:10.1016/j.neuroimage.2014.01.060
45. Cedres N, Ferreira D, Nemy M, et al. Association of Cerebrovascular and Alzheimer Disease Biomarkers With Cholinergic White Matter Degeneration in Cognitively Unimpaired Individuals. *Neurology*. Published online August 2, 2022:10.1212/WNL.0000000000200930. doi:10.1212/WNL.0000000000200930
46. Breiman L. Random forests. *Mach Learn*. 2001;45(1):5-32. doi:10.1023/A:1010933404324
47. Breiman L. Bagging predictions. *Mach Learn*. 1996;24(2):123-140. doi:10.1023/A:1018054314350
48. Lebedev A V., Westman E, Van Westen GJP, et al. Random Forest ensembles for detection and prediction of Alzheimer's disease with a good between-cohort robustness. *NeuroImage Clin*. 2014;6:115-125. doi:10.1016/j.nicl.2014.08.023
49. Strobl C, Boulesteix AL, Zeileis A, Hothorn T. Bias in random forest variable importance

measures: Illustrations, sources and a solution. *BMC Bioinformatics*. 2007;8. doi:10.1186/1471-2105-8-25

50. Robin X, Turck N, Hainard A, et al. pROC: An open-source package for R and S+ to analyze and compare ROC curves. *BMC Bioinformatics*. 2011;12(1):77. doi:10.1186/1471-2105-12-77

51. Lin C-P, Frigerio I, Boon BDC, et al. Structural (dys)connectivity associates with cholinergic cell density in Alzheimer's disease. *Brain*. 2022;145(8):2869-2881. doi:10.1093/brain/awac093

52. Wolfsgruber S, Kleineidam L, Guski J, et al. Minor neuropsychological deficits in patients with subjective cognitive decline. *Neurology*. 2020;95(9):e1134-e1143. doi:10.1212/WNL.0000000000010142

53. Rami L, Fortea J, Bosch B, et al. Cerebrospinal fluid biomarkers and memory present distinct associations along the continuum from healthy subjects to AD patients. *J Alzheimer's Dis*. 2011;23(2):319-326. doi:10.3233/JAD-2010-101422

54. Visser PJ, Verhey F, Knol DL, et al. Prevalence and prognostic value of CSF markers of Alzheimer's disease pathology in patients with subjective cognitive impairment or mild cognitive impairment in the DESCRIPA study: a prospective cohort study. *Lancet Neurol*. 2009;8(7):619-627. doi:10.1016/S1474-4422(09)70139-5

55. Antonell A, Fortea J, Rami L, et al. Different profiles of Alzheimer's disease cerebrospinal fluid biomarkers in controls and subjects with subjective memory complaints. *J Neural Transm*. 2011;118(2):259-262. doi:10.1007/s00702-010-0534-0

56. Sánchez-Benavides G, Suárez-Calvet M, Milà-Alomà M, et al. Amyloid-β positive individuals with subjective cognitive decline present increased CSF neurofilament light levels that relate to lower hippocampal volume. *Neurobiol Aging*. 2021;104:24-31. doi:10.1016/j.neurobiolaging.2021.02.026

57. Ferreira D, Falahati F, Linden C, et al. A "Disease Severity Index" to identify individuals with Subjective Memory Decline who will progress to mild cognitive impairment or dementia. *Sci Rep*. 2017;7. doi:10.1038/srep44368

58. Ebenau JL, Pelkmans W, Verberk IMW, et al. Association of CSF, Plasma, and Imaging Markers of Neurodegeneration with Clinical Progression in People with Subjective Cognitive Decline. *Neurology*. 2022;98(13):E1315-E1326.

doi:10.1212/WNL.0000000000200035

59. Schmitz TW, Nathan Spreng R. Basal forebrain degeneration precedes and predicts the cortical spread of Alzheimer's pathology. *Nat Commun*. 2016;7(1):1-13. doi:10.1038/ncomms13249

60. Cicognola C, Hansson O, Scheltens P, et al. Cerebrospinal fluid N-224 tau helps discriminate Alzheimer's disease from subjective cognitive decline and other dementias. *Alzheimer's Res Ther*. 2021;13(1). doi:10.1186/s13195-020-00756-6

61. Sun X, Salat D, Upchurch K, Deason R, Kowall N, Budson A. Destruction of white matter integrity in patients with mild cognitive impairment and Alzheimer disease. *J Investig Med*. 2014;62(7):927-933. doi:10.1097/JIM.0000000000000102

62. Teipel S, Heinsen H, Amaro E, et al. Cholinergic basal forebrain atrophy predicts amyloid burden in Alzheimer's disease. *Neurobiol Aging*. 2014;35(3):482-491. doi:10.1016/j.neurobiolaging.2013.09.029

63. Lee PL, Chou KH, Chung CP, et al. Posterior Cingulate Cortex Network Predicts Alzheimer's Disease Progression. *Front Aging Neurosci*. 2020;12:466. doi:10.3389/fnagi.2020.608667

64. Palmqvist S, Schöll M, Strandberg O, et al. Earliest accumulation of β-amyloid occurs within the default-mode network and concurrently affects brain connectivity. *Nat Commun*. 2017;8(1):1-13. doi:10.1038/s41467-017-01150-x

65. Coughlan G, Laczó J, Hort J, Minihane AM, Hornberger M. Spatial navigation deficits — Overlooked cognitive marker for preclinical Alzheimer disease? *Nat Rev Neurol*. 2018;14(8):496-506. doi:10.1038/s41582-018-0031-x

66. Fernández-Cabello S, Kronbichler M, van Dijk KRA, Goodman JA, Nathan Spreng R, Schmitz TW. Basal forebrain volume reliably predicts the cortical spread of Alzheimer's degeneration. *Brain*. 2020;143(3):993-1009. doi:10.1093/brain/awaa012

67. Schulz J, Pagano G, Fernández Bonfante JA, Wilson H, Politis M. Nucleus basalis of Meynert degeneration precedes and predicts cognitive impairment in Parkinson's disease. *Brain*. 2018;141(5):1501-1516. doi:10.1093/brain/awy072

68. Nishioka C, Liang HF, Barsamian B, Sun SW. Amyloid-beta induced retrograde axonal degeneration in a mouse tauopathy model. *Neuroimage*. 2019;189:180-191. doi:10.1016/j.neuroimage.2019.01.007

69. Teipel SJ, Kuper-Smith JO, Bartels C, et al. Multicenter Tract-Based Analysis of Microstructural Lesions within the Alzheimer's Disease Spectrum: Association with Amyloid Pathology and Diagnostic Usefulness. *J Alzheimers Dis*. 2019;72(2):455-465. doi:10.3233/JAD-190446

Figure legends

Figure 1 Parameters of diffusivity in cholinergic pathways and remaining WM. All clinical groups differed in FA and MD compared to the HC groups in all observed pathways. **(A)** Average FA. **(B)** Average MD. ns, not statistically significant ($p > 0.05$), *$p < 0.05$, **$p < 0.01$, ***$p < 0.001$ (assessed using a two-tailed alpha). FA, fractional anisotropy; MD, mean diffusivity; HC, healthy controls; SCD, subjective cognitive decline MCI, mild cognitive impairment; AD, Alzheimer's disease dementia.

Figure 2 Voxel-wise differences in mean diffusivity (MD) between diagnostic groups and controls (cingulum pathway), controlling for age and sex. The cingulum pathway showed significantly higher MD values in the posterior/retrosplenial cingulate already in the SCD group compared with the HC group. Additional differences were present in the rostral and dorsal anterior cingulate in MCI and AD dementia groups. Voxel-wise analyses of the diffusion data (MD values) were performed using non-parametric permutation testing. Identification of significant clusters in the data was performed using threshold-free cluster enhancement (TFCE). Significance maps were corrected for multiple comparisons using a familywise error rate of $p < 0.05$ (non-significant voxels are shown in green). BF mask (in purple) was inflated for

illustrative purposes. HC, healthy controls; SCD, subjective cognitive decline; MCI, mild cognitive impairment; AD, Alzheimer's disease dementia.

Figure 3 Voxel-wise difference in mean diffusivity (MD) between diagnostic groups and controls (external capsule pathway), controlling for age and sex. The external capsule pathway showed differences in the external capsule, posterior/retrosplenial cingulate, and parts of the uncinate fasciculus in SCD and MCI compared with HC. Additional differences were present in temporal and prefrontal areas in the AD dementia group. Voxel-wise analyses of the diffusion data (MD values) were performed using non-parametric permutation testing. Identification of significant clusters in the data was performed using threshold-free cluster enhancement (TFCE). Significance maps were corrected for multiple comparisons using a familywise error rate of $p < 0.05$ (statistically non-significant voxels are shown in green). BF mask (in purple) was inflated for illustrative purposes. HC, healthy controls; SCD, subjective cognitive decline; MCI, mild cognitive impairment; AD, Alzheimer's disease dementia.

Figure 4 Random Forest models (increase in prediction error). In the normal cognition groups (HC and SCD), MD in the external capsule pathway was important in predicting scores in attention tests, while NBM volume and WM-hypointensities received low importance scores in all models. In the impaired cognition groups (MCI and AD dementia), NBM volume and MD in external capsule and cingulum pathways were important in predicting scores in most memory and attention tests. MD, mean diffusivity; ExCap, external capsule pathway; Cing, cingulum pathway; Rem WM, WM excluding cholinergic pathways; NBM/TIV, volume of nucleus basalis

of Meynert scaled by total intracranial volume; Var, variance; yrs, years. IncMSE, conditional variable importance computed by increase in the mean square error of prediction. This IncMSE is the result of a corresponding variable being permuted within a grid defined by the covariates that are associated to the variable of interest.

Figure 5 Receiver operating characteristic (ROC) curves for diffusion and conventional MRI biomarkers. The figures show that cholinergic WM pathways outperformed other MRI biomarkers in the SCD group, and that all considered biomarkers performed better with a more advanced clinical stage of the disease in the AD continuum, in distinguishing between a clinical group and HC. *$p < 0.05$, **$p < 0.01$, ***$p < 0.001$ (assessed using a two-tailed alpha). MD, mean diffusivity; HC, healthy controls; SCD, subjective cognitive decline; MCI, mild cognitive impairment; AD, Alzheimer's disease dementia; MD, mean diffusivity; ExCap, external capsule pathway; Cing, cingulum pathway; Rem WM, WM excluding cholinergic pathways; NBM vol., volume of nucleus basalis of Meynert scaled by total intracranial volume; hippocampus vol., volume of hippocampus scaled by total intracranial volume.

Table 1 Demographic and clinical variables by group

	Whole sample	HC	SCD	MCI	AD dementia	*F*-value/χ^2-value
n	402	112	172	66	52	
age	71.5 (6.5) [59–89]	69.1 (5.6) [60–81]	71.6 (6.3)** [59–87]	72.6 (6.4)** [61–86]	75.2 (6.8)*** [60–89]	12.6, $p < 0.001$
sex (M/F)	210/192	48/64	96/76*	43/23**	23/29^{ns}	10.6, $p < 0.05$
years of education	14.3 (3.0)	14.8 (2.7)	14.5 (3.0)^{ns}	14.1 (3.1)^{ns}	12.6 (3.0)***	6.9, $p < 0.001$
MMSE total score	28.1 (2.9)	29.4 (0.9)	29.2 (0.9)^{ns}	27.8 (1.8)***	21.9 (3.1)***	324, $p < 0.001$
ADAS word list learning (immediate recall)	19.8 (5.5)	23.2 (3.5)	21.6 (3.7)^{ns}	16.4 (3.9)***	10.7 (4.0)***	151, $p < 0.001$
ADAS word list recall (delayed recall)	6.20 (2.95)	8.09 (1.62)	7.23 (1.78)*	4.03 (2.44)***	1.24 (1.61)***	191, $p < 0.001$
ADAS figure learning (recall)	8.35 (3.40)	9.99 (1.60)	9.78 (1.79)^{ns}	6.64 (3.22)***	1.98 (2.18)***	201, $p < 0.001$
Trail making test A	51.0 (30.3)	43.9 (17.3)	41.0 (14.7)^{ns}	57.0 (27.1)*	94.2 (52.2)***	52.0, $p < 0.001$
Trail making test B	116.6 (62.8)	90.5 (25.8)	101.0 (38.4)^{ns}	133.0 (60.7)***	244.0 (84.0)***	100, $p < 0.001$
Symbol digit modalities test	42.4 (13.3)	49.6 (9.2)	45.7 (9.8)^{ns}	37.3 (9.8)***	21.2 (12.0)***	90.0, $p < 0.001$
NBM volume (µl) (TIV corrected)	236 (68)	272 (50)	246 (61)*	208 (62)***	160 (58)***	39.1, $p < 0.001$
hippocampal volume (µl) (TIV corrected)	6000 (1100)	6680 (870)	6200 (1100)*	5430 (950)***	4790 (870)***	43.9, $p < 0.001$
WMH load (µl)	3954 (4826)	2421 (3311)	3516 (3870)^{ns}	5071 (5654)*	7285 (7039)***	9.7, $p < 0.001$
APOE genotype, n	388	109	166	63	50	
APOE4 genotype, n (%)	132 (34.0)	24 (22.0)	51 (30.7)^{ns}	30 (47.6)***	27 (54.0)***	21.9, $p < 0.001$
CSF biomarkers, n	185	40	73	47	25	
Aβ42/Aβ40	0.079 (0.029)	0.097 (0.023)	0.088 (0.027)^{ns}	0.066 (0.028)***	0.052 (0.017)***	17.3, $p < 0.001$
total tau (pg/ml)	486 (299)	368 (143)	378 (188)^{ns}	544 (257)*	883 (438)***	23.1, $p < 0.001$
p-tau181 (pg/ml)	64.1 (36.7)	51.3 (17.3)	52.5 (24.7)^{ns}	70.1 (31.8)*	107.0 (58.4)***	16.8, $p < 0.001$

Variables in the SCD, MCI, and AD dementia groups were all statistically compared to the corresponding variable in the HC group. For age and years of education an independent *t*-test was performed. For sex and APOE4 genotype, a chi-square test was performed. For all other variables, one-way ANCOVA were performed by setting a diagnostic group as the independent variable and age and sex as covariates. P-values result from *post hoc* tests between a diagnostic group and HC with Tukey correction for multiple comparisons. ns, not statistically significant ($p > 0.05$), *$p < 0.05$,**$p < 0.01$,***$p < 0.001$ (assessed using a two-tailed alpha). Values reflect mean value (SD) [range] or count. HC = healthy controls; SCD = subjective cognitive decline; MCI = mild cognitive impairment; AD dementia = Alzheimer's disease dementia; M = male; F = female; MMSE = Mini-Mental State Examination; ADAS = The Alzheimer's Disease Assessment Scale; NBM volume = volume of nucleus basalis of Meynert; TIV = total intracranial volume; WHM = white matter hypointensities; CSF = cerebrospinal fluid.

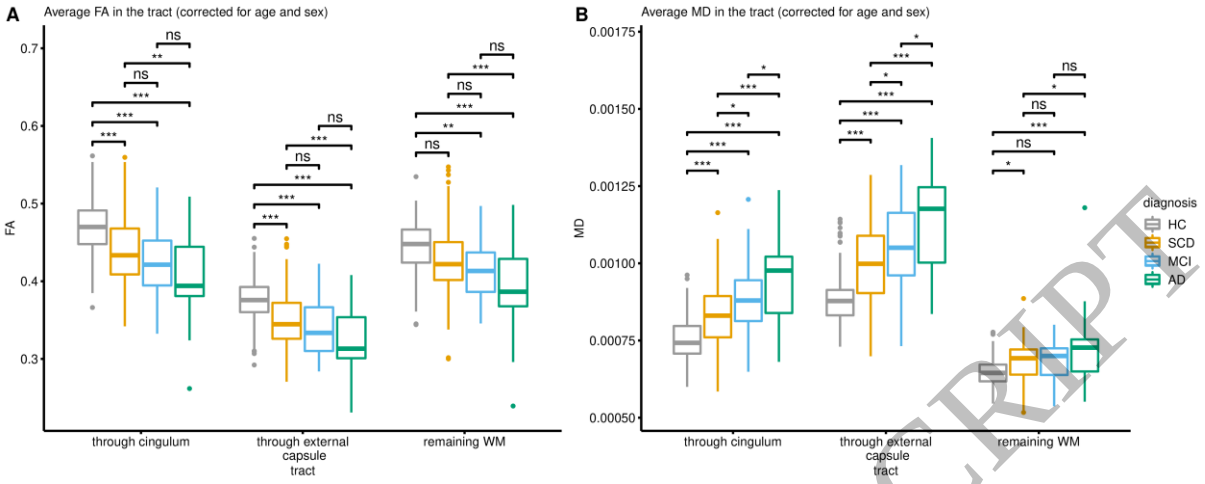

Figure 1
159x64 mm (1.0 x DPI)

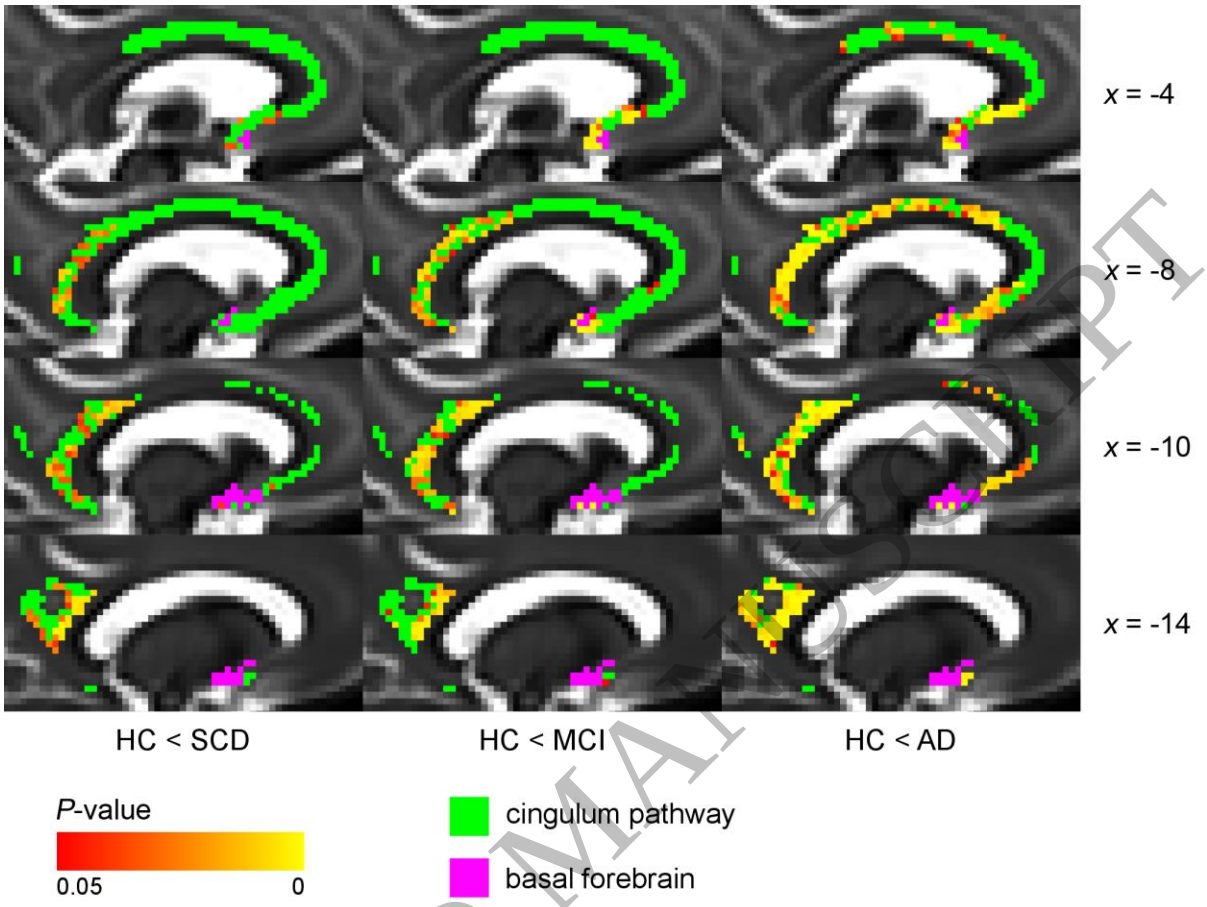

Figure 2
159x120 mm (1.0 x DPI)

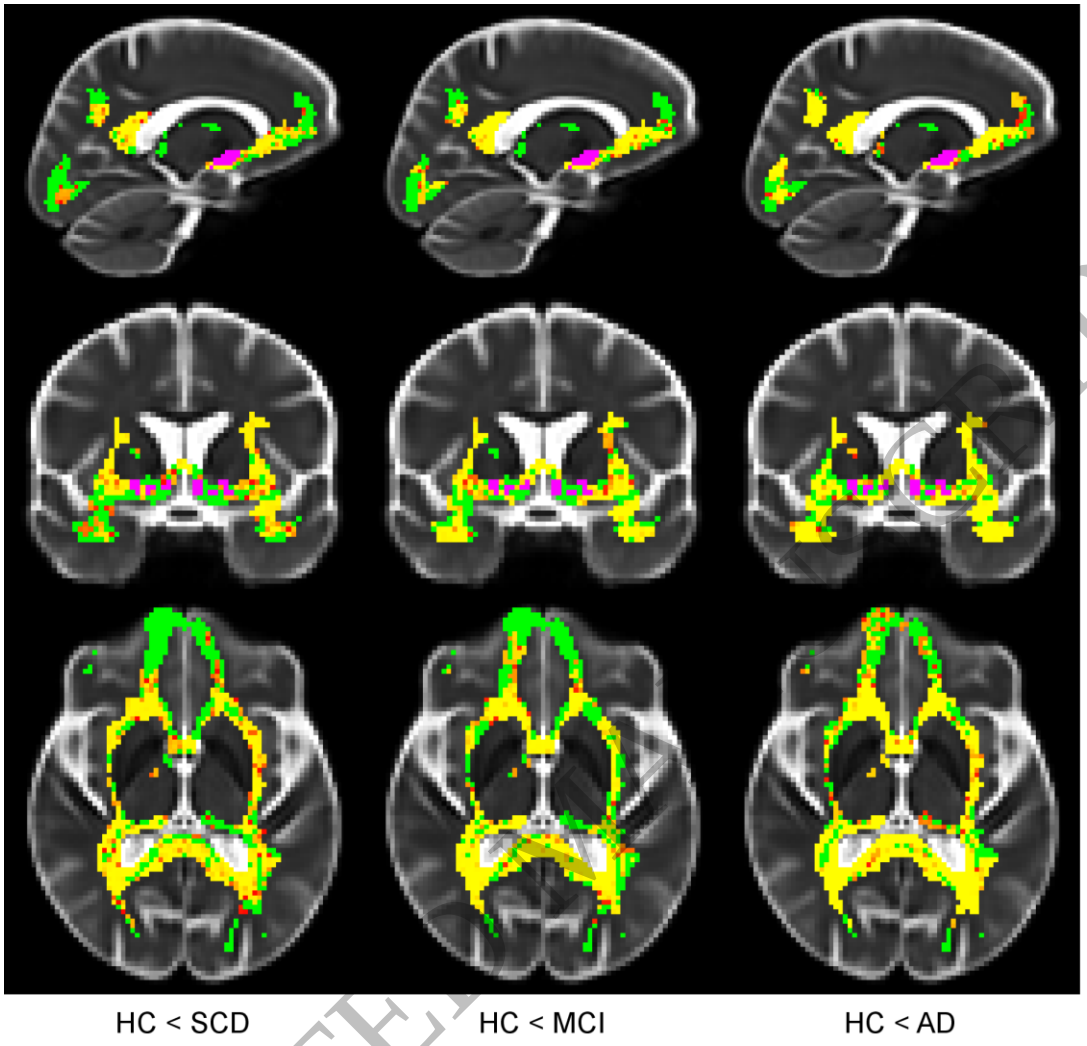

Figure 3
159x157 mm (1.0 x DPI)

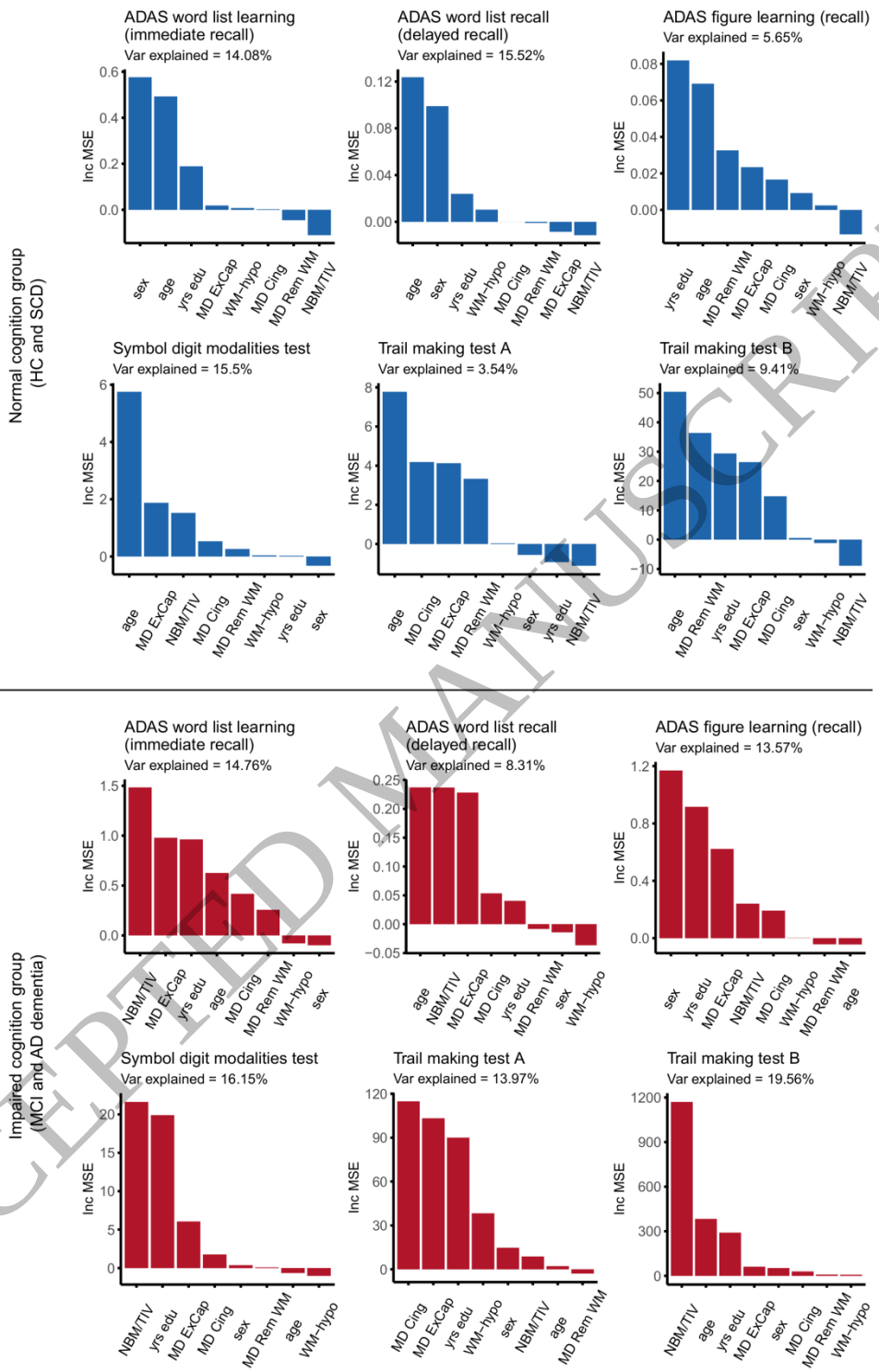

Figure 4
159x245 mm (1.0 x DPI)

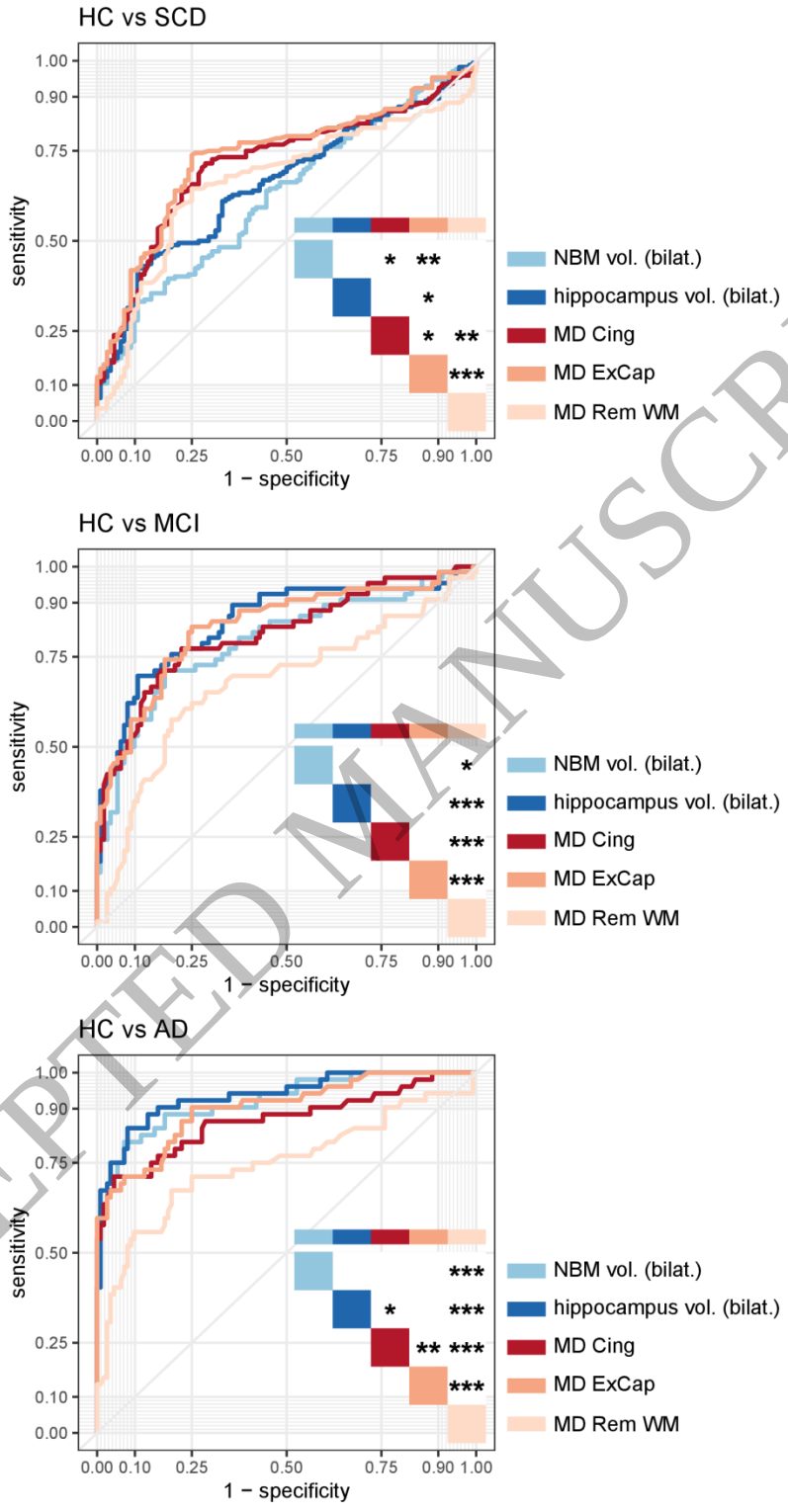

Figure 5
127x246 mm (1.0 x DPI)